Colloids and Surfaces B: Biointerfaces 267 (2026) 115892

Contents lists available at ScienceDirect

Colloids and Surfaces B: Biointerfaces

journal homepage: www.elsevier.com/locate/colsurfb

Liposome formulation of a myristoylated antimicrobial peptide derived from Chionodracine: preparation, physico-chemical characterization and biological activity

Federica Toma [a,1], Antonia Volpe [a], Fabiana Pandolfi [b], Federica Massaro [c], Fernando Porcelli [c], Francesco Buonocore [c], Anna Rita Taddei [d], Damiano Squitieri [e,f], Francesca Bugli [e,f], Francesca Ceccacci [b], Stefano Borocci [b,c,*], Mariangela Clemente [b,*], Cecilia Bombelli [b]

[a] Sapienza University of Rome, P.le A. Moro 5, Rome 00185, Italy
[b] Institute for Biological Systems (ISB), National Research Council of Italy (CNR), Secondary Office of Rome-Reaction Mechanisms c/o Department of Chemistry, Sapienza University of Rome, P.le A. Moro 5, Rome 00185, Italy
[c] Department for Innovation in Biological, Agro-Food and Forest Systems (DIBAF), University of Tuscia, L.go dell'Università, s.n.c, Viterbo 01100, Italy
[d] Center of Large Equipments, Section of Electron Microscopy, University of Tuscia, L.go dell'Università, s.n.c, Viterbo 01100, Italy
[e] Department of Basic Biotechnological Sciences, Intensive and Perioperative Clinics, Catholic University of the Sacred Heart, Rome, Italy
[f] Department of Laboratory Sciences and Infectious Diseases, A. Gemelli University Hospital Foundation IRCCS, Rome, Italy

ARTICLE INFO

Keywords:
Liposomes
CHEMS
Lipopeptide
Antifungal activity
Antibiofilm activity
Molecular dynamics simulations

ABSTRACT

Second-generation antimicrobial lipopeptides are considered very promising tools to combat the spread of systemic fungal infections caused by fungi multidrug resistance and biofilm-associated infections. The present work reports a study on the lipopeptide Myr-B, derived from myristoylation of the natural antimicrobial peptide Chionodracine. The aim was to exploit its therapeutic potential by developing a suitable procedure for its encapsulation in liposomes, with a view to overcoming its *in vivo* instability and tendency to aggregation. A systematic investigation allowed to select two optimal liposome formulations, based on dimyristoylphosphatidylcholine, having chains of the same length of the lipopetide, and cholesterol and/or cholesteryl-hemisuccinate. Thin-film hydration and lipid-cake preparation methods were explored, and chemical-physical characterization was integrated with molecular dynamics simulations. The lipid-cake method proved to be the optimal approach, yielding monodisperse, stable liposomes with high encapsulation efficiency. Encapsulation in both liposome formulations markedly enhanced antifungal activity, lowering minimum inhibitory concentrations more than ten-fold against *Candida albicans* and approximately four-fold against *Candida tropicalis* compared to free Myr-B. LIVE/DEAD imaging also confirmed a strong reduction in biofilm formation. Liposomes displayed minimal haemolysis, low cytotoxicity toward human fibroblasts, and good *in vivo* tolerability in *Galleria mellonella*. Notably, specific interactions between cholesteryl-hemisuccinate and the peptide involved a peculiar liposome structure and a slower release from the liposome. Overall, both Myr-B–loaded liposomes produced by the lipid cake protocol significantly potentiates MYR-B efficacy while maintaining a favourable safety profile. These formulations are not universally applicable to all lipopeptides; however, the underlying criteria presented in this work are.

* Correspondence to: Stefano Borocci at Department for Innovation in Biological, Agro-Food and Forest Systems (DIBAF), University of Tuscia, L.go dell'Università, s.n.c., 01100 Viterbo (Italy); Mariangela Clemente at Institute for Biological Systems (ISB), National Research Council of Italy (CNR), Secondary Office of Rome-Reaction Mechanisms c/o Department of Chemistry, Sapienza University of Rome, P.le A. Moro 5, Rome 00185, Italy.
E-mail addresses: borocci@unitus.it (S. Borocci), mariangela.clemente@cnr.it (M. Clemente).
[1] Present affiliation: Department of Translational Medicine and Surgery, Università Cattolica del Sacro Cuore 00168 Rome, Italy

https://doi.org/10.1016/j.colsurfb.2026.115892
Received 20 March 2026; Received in revised form 4 June 2026; Accepted 5 June 2026
Available online 13 June 2026

1. Introduction

Since the early 21st century, research efforts to develop antimicrobial peptides (AMPs) have intensified considerably due to the outbreak of antimicrobial resistance (AMR) and the emergence of multidrug-resistance (MDR) [1]. At present, AMPs are considered among the most promising tools to fight against multidrug resistance of pathogens and biofilm-associated infections, thanks to their mechanism of action which is generally different from that of traditional antibiotics.

The presence of certain AMPs on the market attests to their effectiveness: some are highly active against Gram-positive and Gram-negative bacteria [2] and fungi that are resistant to traditional antibiotics [3].

These AMPs are all first-generation AMPs, *i.e.* extracted from bacteria or obtained through simple synthetic modifications of natural AMPs. Despite their efficacy, many of them exhibit severe toxicity, especially nephrotoxicity, mainly because high doses are required due to poor bioavailability [4]. As an example, colistin is only used as a last resort just because of its toxicity. To further complicate the situation, although it was presumed for years that AMPs could not induce resistance as their action is disrupting pathogen cell membrane, bacterial strains resistant to vancomycin and even colistin are now being found [5,6]. A similar scenario is observed for approved AMPs with antifungal activity, which are highly toxic to the liver and can cause allergic reactions (caspofungin) [7].

An increasing number of fungi are now resistant to traditional drugs, as demonstrated by the increasing number of fungal pathogens added to the Centres for Disease Control and Prevention Antimicrobial Resistance Threats Report in 2019 [8]. Since systemic fungal infections are very dangerous and are becoming increasingly common with respect to topical ones, particularly in immunocompromised patients [9], the need for more effective and less toxic antifungal drugs is undeniable.

Several strategies are currently being investigated to address this crucial objective, including the formulation of drugs (both existing and newly developed) into suitable nanocarriers with the aim of improving bioavailability, enhancing therapeutic efficacy, reducing drug-associated toxicity, and bypassing resistance mechanisms [10].

Starting from data collected on natural AMPs concerning the correlation between peptide sequence and activity as well as between peptide sequence and toxicity, researchers developed second-generation AMPs. These AMPs were designed to be less toxic to the self, more pathogen-specific, soluble, bioavailable, and stable in biological fluids. In particular, to increase the antifungal activity of AMPs, a valid approach was their conjugation with a lipophilic chain of fatty acids [11,12]. Thanks to the rational design, some second-generation AMPs are already in clinical trial. Unfortunately, among these, only three possess antifungal activity and of these two are being studied only for topical application [2].

As early as the end of the last century, many nano-sized drug delivery systems, such as dendrimers, liposomes, lipid-based systems, micelles, hydrogels, nanocrystal, carbon nanomaterials, inorganic metallic and polymeric nanoparticles, have been investigated to address the limitations of conventional antimicrobial drugs and AMPs [13,14]. Many antifungal drugs have been incorporated into different types of nano-delivery systems which have been shown to increase the activity and solubility of drugs while reducing their toxicity [3].

In this vast scenario of nano-platforms, liposomes showed many advantages in antimicrobial therapies in terms of biocompatibility, biodegradability, increased solubility of antibiotics [15–17] as well as enhanced accumulation at infection sites, local increases in antibiotic concentration, and activity against intracellular pathogens [18]. The literature also reports liposomal formulations that have been shown to enhance the efficacy of the AMPs against both bacteria and fungi [19–21].

In the present study was investigated the encapsulation in liposomes of the lipopeptide $CH_3(CH_2)_{12}$COWRGITKVVKKV (Myr-B), with the aim of enhancing its already proved activity against *Candida spp* [22,23], while overcoming its instability *in vivo* and tendency to aggregation. A neutral (DMPC/Chol) and a negatively charged (DMPC/Chol/CHEMS) formulation were developed (Chart 1). Liposomes' morphology and physico-chemical properties were investigated by different experimental techniques. Molecular Dynamics (MD) simulations were carried out to investigate, with an atomic resolution, the interaction of Myr-B with lipids, its insertion into the liposomal bilayer, and its effect on bilayer's organization. Haemolytic activity and toxicity were investigated, both *in vitro* and *in vivo*, using *Galleria mellonella* larvae as a model. Antifungal activity was evaluated against two *Candida* species, on both the planktonic and biofilm form. *Candida albicans* remains the predominant etiological agent of invasive candidiasis worldwide, accounting for approximately 40–50% of clinical isolates across most geographic regions, and has long been regarded as the reference species for antifungal susceptibility testing [24]. Although *C. albicans* retains its position as the most frequently isolated *Candida* species, non-*albicans Candida* (NAC) species now account for a substantial proportion of clinical isolates recovered globally in hospital settings, with *C. tropicalis* being among those of greatest clinical concern [25,26]. *Candida tropicalis* ranks among the most important NAC species in terms of epidemiology, virulence, and antifungal resistance, and has been consistently described as one of the most adherent and robust biofilm-producing *Candida* species [27–29]. On these grounds, *C. albicans* and *C. tropicalis* were selected as representative test organisms to assess the antifungal activity of the Myr-B loaded liposomes, encompassing both the archetypical *Candida* pathogen and a clinically significant, biofilm-proficient NAC species.

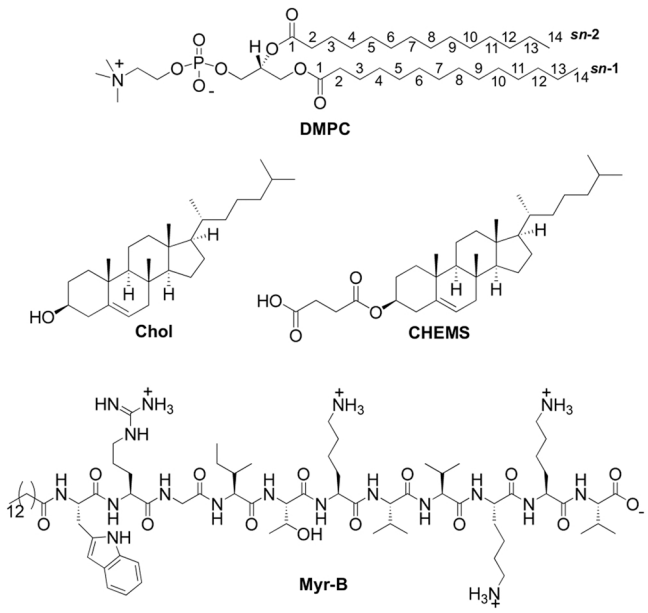

Chart 1. Molecular Structure of lipids and Myr-B lipopeptide.

2. Results and discussion

In order to develop stable monodisperse vesicles with good Myr-B encapsulation rate, the lipid composition, the total concentration of the components, and the lipid/peptide molar ratio were properly modulated finally selecting two formulations, namely DMPC/Chol and DMPC/Cholesteryl-hemisuccinate (CHEMS), at 1.9 mM total lipid concentration and 1:30 lipopeptide/lipids ratio. These concentrations represent the optimal ones to have stable liposomes with the higher entrapment of Myr-B. The studies previously performed to identify the final formulations are reported in the SI [30]. From these studies, DMPC emerged as the best choice due to its acyl chains having the same length

as that of Myr-B, allowing the formation of a more homogeneous and compact lipid bilayer. Since high concentrations of Chol are reported to reduce the trapping efficiency of AMPs [31], a small amount of Chol (5%) was included to obtain monodisperse liposomes stable for a few days without compromising encapsulation efficiency.

The ionizable cholesterol derivative CHEMS is utilised in the preparation of liposomes for the delivery of antibacterial drugs [32,33] because of its fusogenic properties, responsiveness to pH [34,35], ability of stabilizing proteins and compacting the lipid bilayers [36]. In this work it was incorporated into one liposome bilayer with the objective of enhancing the stability of the formulation. To evaluate the effect of the preparation protocol on the physico-chemical properties of Myr-B-loaded liposomes, the lipid cake method (hydration of a freeze-dried monophase system) was compared with the standard thin film hydration (TFH) method (hydration of a thin lipid/peptide film with the buffer); the LC method was chosen because already reported as particularly suitable for promoting a better incorporation of lipopeptides into the liposome bilayer [37]. The results of this investigation are presented in Table 1.

Freshly prepared liposomes, empty or loaded with Myr-B, are monodisperse and with diameter consistent with those of the pores of the extrusion membrane. Myr-B loaded liposomes with CHEMS resulted smaller (Table 1) and less stable upon time (see Figure S1 and S2 of the SI [30]) than the ones without CHEMS. Replacing Chol with CHEMS had a remarkable effect on liposome size only in the presence of the peptide, probably due to the interaction of the negatively charged polar headgroups of CHEMS with the positive moieties of the peptide, resulting in a compaction of the bilayer.

When a substantial percentage of the positively charged peptide was incorporated in the bilayer, the liposome potential shifted to slightly positive values, compared to the negative (DMPC/Chol/CHEMS) or weakly negative (DMPC/Chol) potential of the empty liposomes.

The LC method proved to be better than the TFH one in terms of encapsulation efficiency: the extrusion was faster and more straightforward in the case of LC method compared to the TFH one where increasing the temperatures was required. The superior performance of the LC approach can be attributed to the more homogeneous distribution of the lipopeptide within the lipid matrix achieved by freeze drying. On the contrary, solvent evaporation in the thin-film method leads to a less uniform dispersion [31]. Myr-B-loaded liposomes with and without CHEMS have the same EE%, even if the release over time of the lipopeptide from the liposomes is lower in the presence of CHEMS. (See Figure S3 of SI) These results suggest a specific interaction between the cationic residue of the peptide and the carboxylate group of the CHEMS.

The morphology of both empty and Myr-B-loaded liposomes was studied by transmission electron microscopy (TEM).

Empty DMPC/Chol liposomes (Fig. 1A) exhibited good contrast, a homogeneous surface, and dimensions consistent with DLS (130 nm). Myr-B-loaded DMPC/Chol liposomes (Fig. 1B) showed a less smooth surface together with small membrane cracks (indicated by arrows). This is suggestive of a less compact bilayer more sensitive to perturbation caused by TEM deposition.

Empty DMPC/Chol/CHEMS liposomes exhibited a uniform surface (see Fig. 1C), although some multilamellar structures were observed (see Fig. 1C, inset). In the presence of Myr-B, however, all liposomes became multilamellar, resembling cartellate (a traditional Christmas pastry from southern Italy) (see Fig. 1D, inset) with minor membrane fractures similar to those of DMPC/Chol vesicles (indicated by arrows). Overall, Myr-B strongly affects bilayer organization, with formulation-dependent differences likely arising from peptide–lipid interactions that promote distinct peptide secondary structures in the presence of CHEMS.

The molecular dynamics simulations presented in the next paragraph were conducted to investigate the effect of CHEMS in the bilayer organization and to support the evidence of structural differences evidenced by TEM.

2.1. Molecular dynamics simulations

In order to investigate, with atomic resolution, the structure and organization of Myr-B in lipid membrane of DMPC/Chol and DMPC/Chol/CHEMS, molecular dynamics simulations were performed according to the minimum bias approach used to study the self-assembling of lipids [38] and peptide/membrane complexes [39–41]. Starting from a random orientation of peptides and lipid molecules, the system spontaneously self-assembles in a lipid bilayer allowing the peptide to adopt the most favourable position and orientation into the lipid membrane.

In all simulated systems the formation of lipid bilayer was observed within 150 ns of MD trajectories (Figure S4 and S5) [30] and remains stable for the remaining 2 μs of simulations.

The deuterium order parameter, S_{CD}, of each methylene of lipid alkyl chains was calculated to determine the effects of lipopeptide on the structure of the membrane. The value of $|S_{CD}|$, is indicative of the fluidity of lipid bilayer; the higher the value of $|S_{CD}|$, the more ordered the lipid membrane. A value of $|S_{CD}|$ of 0.5 is characteristic of alkyl chain in all trans conformation and perfectly oriented with respect to the bilayer normal, whereas a value of zero indicates an isotropic orientation of the alkyl chain [42].

Fig. 2A and 2B show the averaged order parameters, $|S_{CD}|$, of the methylene groups of *sn*−1 and *sn*−2 DMPC alkyl chains for the lipid membranes, in absence and in presence of Myr-B.

In the absence of peptides, the bilayer of DMPC/Chol and DMPC/CHEMS showed the same profile of $|S_{CD}|$ for the alkyl chains of DMPC, with only small difference for the first four methylenes of *sn*−2 chain.

In the presence of four molecules of Myr-B, the DMPC/Chol membrane showed a lower value of $|S_{CD}|$ (higher mobility) with respect to DMPC/CHEMS membrane for the first seven methylenes of *sn*−1 chain (Fig. 2A) and all methylenes of DMPC *sn*-2 chain (Fig. 2B). In the case of *sn*-1 chains the terminal eight methylenes of DMPC/Chol and DMPC/CHEMS membranes shows the same value of the order parameter.

The mass density distribution of selected atoms of Myr-B molecules with respect to the lipid bilayer center was calculated to investigate the

Table 1
Physico-chemical properties and Myr-B entrapping efficiency (EE %) of the selected liposomal formulations. Reported data are the average of at least 3 independent experiments, and the error is the standard deviation of three independent measurements.

Formulation	Method	[L] / [P] ratio	D_h (nm)	PDI	ζ (mV)	EE%	[Myr-B] (μM)
DMPC/Chol[a]	LC	-	103 ± 2	0.09 ± 0.01	−0.70 ± 0.01	-	-
DMPC/Chol/CHEMS[b]	LC	-	111 ± 1	0.06 ± 0.01	−5.0 ± 1.0	-	-
Myr-B DMPC/Chol[c]	TFH[d]	30:1	98 ± 2	0.10 ± 0.01	−1.0 ± 1.8	59	38
Myr-B DMPC/Chol/	LC	30:1	101 ± 2	0.10 ± 0.02	3.0 ± 0.5	89	55
Myr-B DMPC/Chol/CHEMS	LC	30:1	106 ± 1	0.08 ± 0.01	3.0 ± 1.0	74	55

[a] [DMPC]= 1.8 mM [Chol]= 0.1 mM;
[b] [DMPC]= 1.8 mM [Chol]= 0.08 mM [CHEMS]= 0.02 mM;
[c] [Myr-B] = 66 μM after hydration of the thin film with PB.
[d] D_h, PDI and ζ-potential of the Myr-B/DMPC/Chol/ formulation prepared by the TFH method, before filtration on sephadex G−50, are D_h = 101 ± 3 nm, PDI= 0.2 ± 0.03, ζ= 6.0 ± 0.07 mV respectively.

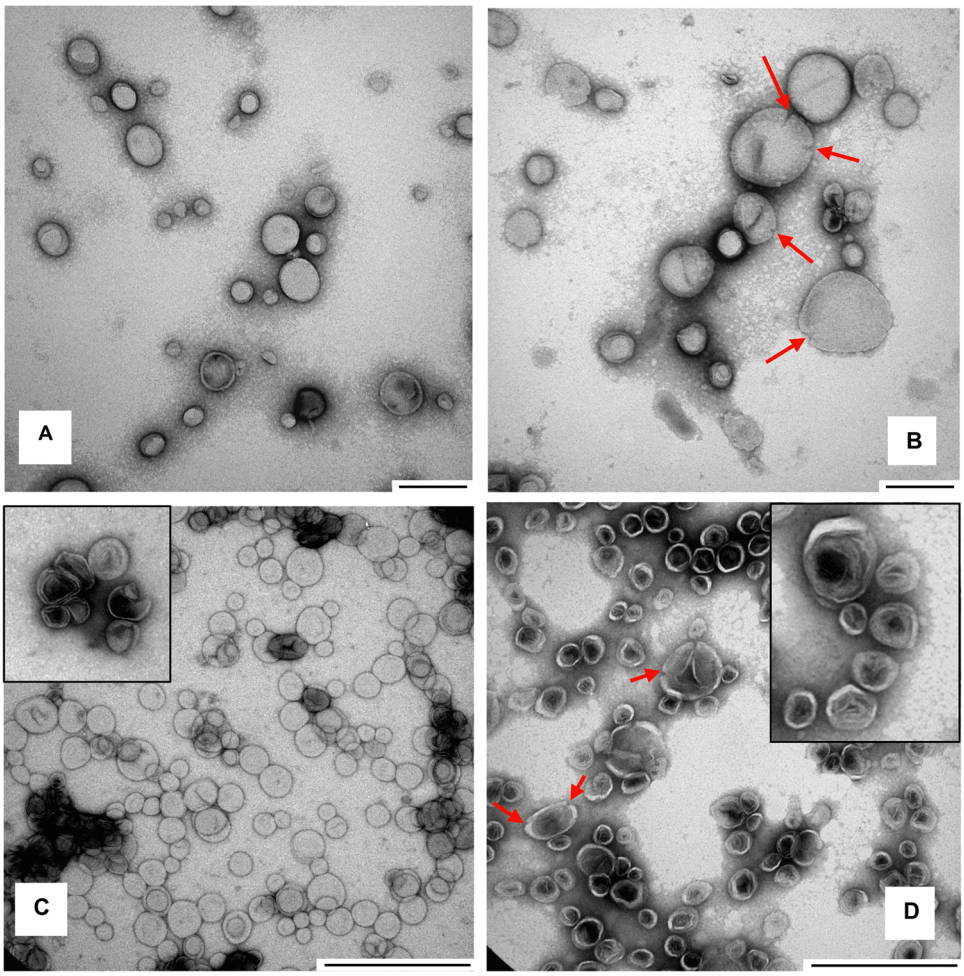

Fig. 1. TEM images of liposomes stained with uranyl acetate: A) DMPC/Chol, B) DMPC/Chol/Myr-B, C) DMPC/Chol/CHEMS, D) DMPC/Chol/CHEMS/Myr-B. Samples in A and B were fixed with OsO_4 (0.025%) while in C and D with PFA.The scale bar placed in the panels corresponds to 200 μm.

organization of the peptide in the lipid bilayer. Fig. 2C and 2D shows the density distributions of phosphorous atoms of DMPC, water and Myr-B atoms. The analysis of mass density evidenced a different location of the Myr-B molecules inserted in the bilayer of DMPC/Chol and DMPC/CHEMS. In DMPC/Chol the peptides were mainly located near one of the two water/lipid surfaces and in the hydrophobic region of bilayer. Only a few atoms of Myr-B were found close to the surface of the second leaflet of the bilayer (Fig. 2C).

In DMPC/CHEMS the peptide molecules presented a more uniform distribution in the lipid bilayer. In fact, as reported in Fig. 2D, the mass density of Myr-B showed the maxima values close to surface of both leaflets of bilayer and in the hydrophobic region.

The presence of Myr-B, and in particular of the charged residues of lysine and arginine into the hydrophobic region of bilayer, induced a perturbation of the membrane. In DMPC/Chol, to neutralize the positive charge of Lys and Arg of Myr-B in the hydrophobic region, some DMPC molecules penetrate in the lipid bilayer with phosphate groups and the choline nitrogen atoms inside the lipid bilayer, orienting alkyl chains parallel to the surface of the bilayer (Fig. 2E). In DMPC/CHEMS the negative charge of carboxylate group present on the sterol molecule contributed to neutralize the positive charges of lysine and arginine and a smaller number of DMPC molecules oriented the phosphate groups within the hydrophobic region (Fig. 2F).

The residues of lysine and arginine within the bilayer induced also the penetration in the hydrophobic region of water molecules that contributed to destabilize the structure of lipid bilayer (Fig. 2E and 2F).

The average thickness, D_{HH}, calculated as the distance between two peaks of phosphorous atom mass density profiles, showed a slight increase for lipid bilayer containing Myr-B. In the absence of peptide, the calculated average thickness for DMPC/Chol and DMPC/CHEMS were 3.44 ± 0.03 nm and 3.44 ± 0.05 respectively (Figure S6). In presence of Myr-B, a slight increase of the thickness was observed with a value of 3.64 ± 0.03 and 3.66 ± 0.02 nm for DMPC/Chol and DMPC/CHEMS respectively (Figure S7).

In order to characterize the local effect of peptides on the structure of bilayer, analysis of the local thickness was carried out, considering the average position of each phosphorous atom of DMPC. As reported in Fig. 3A-B the presence of Myr-B induced a significant perturbation of lipid bilayer with a reduction of bilayer thickness in the region close to the lipopeptide molecules.

The reduction of local thickness induced by Myr-B molecules is more pronounced in DMPC/Chol bilayer, with a lower value of 1.4 ± 0.3 nm, respect to DMPC/CHEMS bilayer where a lower value of 2.1 ± 0.2 nm was observed.

To evaluate the organization of Chol and CHEMS molecules in the lipid bilayer around the lipopeptide molecules the number of contacts between Myr-B and the sterol molecules was calculated.

In DMPC/Chol the number of contacts between the molecules of cholesterol and Myr-B were considerably smaller, 14.0 ± 6.1, with respect to the number of contacts of CHEMS with Myr-B in DMPC/CHEMS, 190.7 ± 37.1. In the DMPC/Chol system, only one MD simulation showed two Myr-B molecules interacting with cholesterol with an occupancy higher than 50%. (Fig. 3C and Table S3) [30]. In the DMPC/CHEMS system, one MD simulation showed two Myr-B molecules

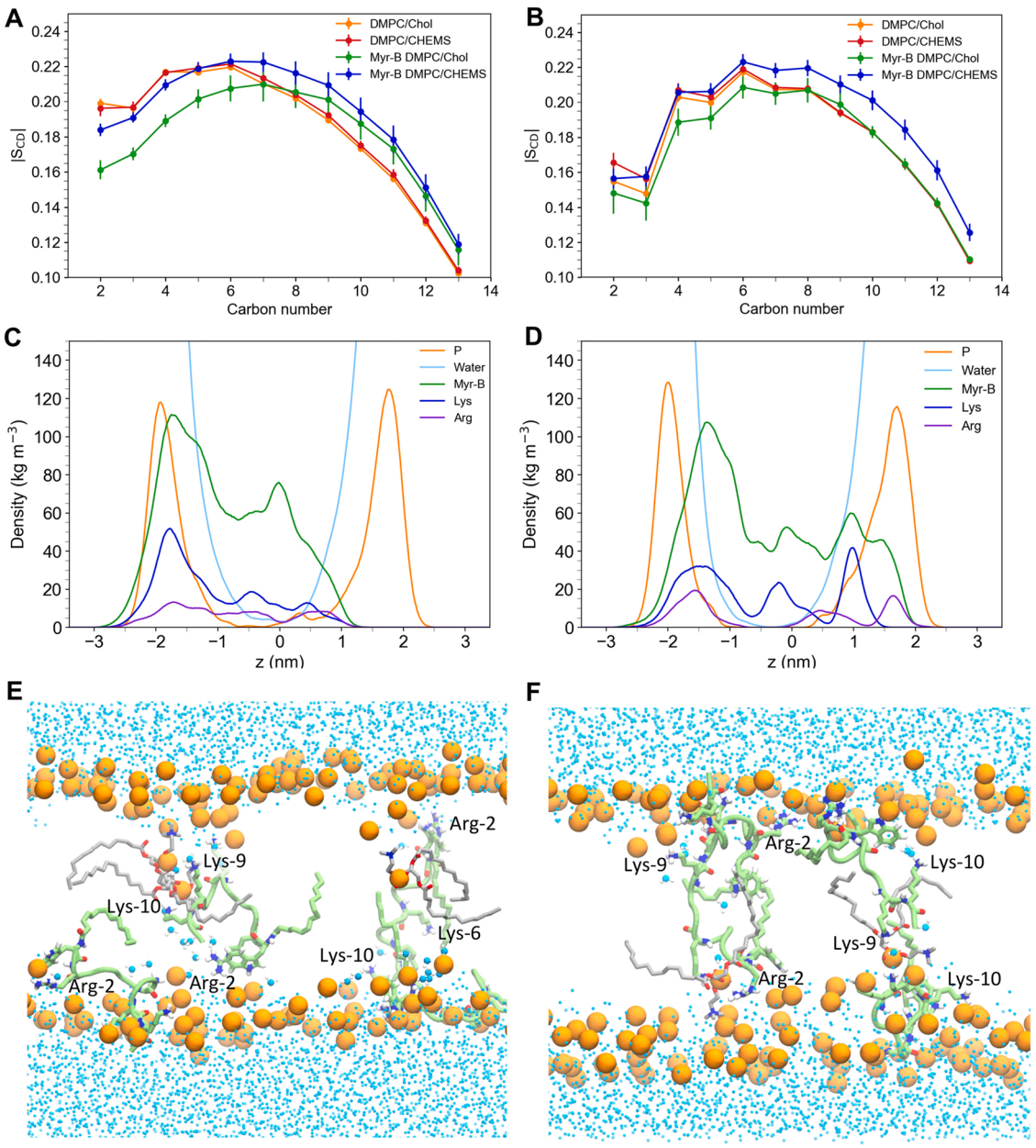

Fig. 2. Deuterium order parameter, $|S_{CD}|$, of **A)** *sn*−1 and **B)** *sn*−2 DMPC alkyl chain in absence and in presence of Myr-B in DMPC/Chol and DMPC/CHEMS membranes. Mass density profiles across the lipid bilayer of phosphorous atoms, water molecules and peptide atoms of **C)** Myr-B in DMPC/Chol and **D)** Myr-B in DMPC/CHEMS. The mass densities are calculated with respect to the center of mass of bilayer (z = 0). Representative structures of **E)** Myr-B in DMPC/Chol and **F)** Myr-B in DMPC/CHEMS. Water oxygens are shown as cyan spheres and phosphorous atoms as orange spheres. The peptide backbone is in green tube, with Arg, Lys, Trp side chains and the myristoyl group in licorice. Nearby DMPC molecules are shown in licorice with grey carbons.

interacting with CHEMS with an occupancy higher than 50%, whereas in the other two simulations, three out of the four Myr-B molecules interacted stably with CHEMS for approximately 1 μs of simulation (Fig. 3C and Table S4) [30].

To further characterize the interaction of the sterol molecules with Myr-B the occupancy of the contacts between the sterol and each residue of lipopeptide was calculated. As shows in Fig. 3D all amino acids of Myr-B, except for Val−11, showed an average value of occupancy for the contact with CHEMS higher than 58%, and for myristoyl alkyl chain, Trp−1, Arg−2, Thr−5 and Lys−6 a value close to 100%. For cholesterol the occupancy of the contacts with the amino acids of Myr-B were significant lower with respect to CHEMS; the myristoyl alkyl chain showed an occupancy of 63% and only the residues Trp−1, Val−7, Lys−10 presented higher occupancy with a value in the range 20–24%.

These data revealed the tendency of CHEMS to organize around the Myr-B and interact stably with the amino acid residues of peptide. The interaction CHEMS/Myr-B was mainly driven by the formation of salt-bridge between the carboxylate group of CHEMS and the positive charged lysine and arginine residues of Myr-B. On the contrary, the molecules of cholesterol presented a lower tendency to organize around the Myr-B molecules (Fig. 3E).

2.2. *Antifungal activity, minimum inhibitory concentration (MIC)*

The antifungal efficacy of Myr-B and Myr-B-loaded liposomes was evaluated, according to EUCAST standard, on *C.tropicalis* and *C.albicans,* the most common pathogenic determinant between *Candida spp.* in hospital-acquired infection [32,33]. The results suggested that

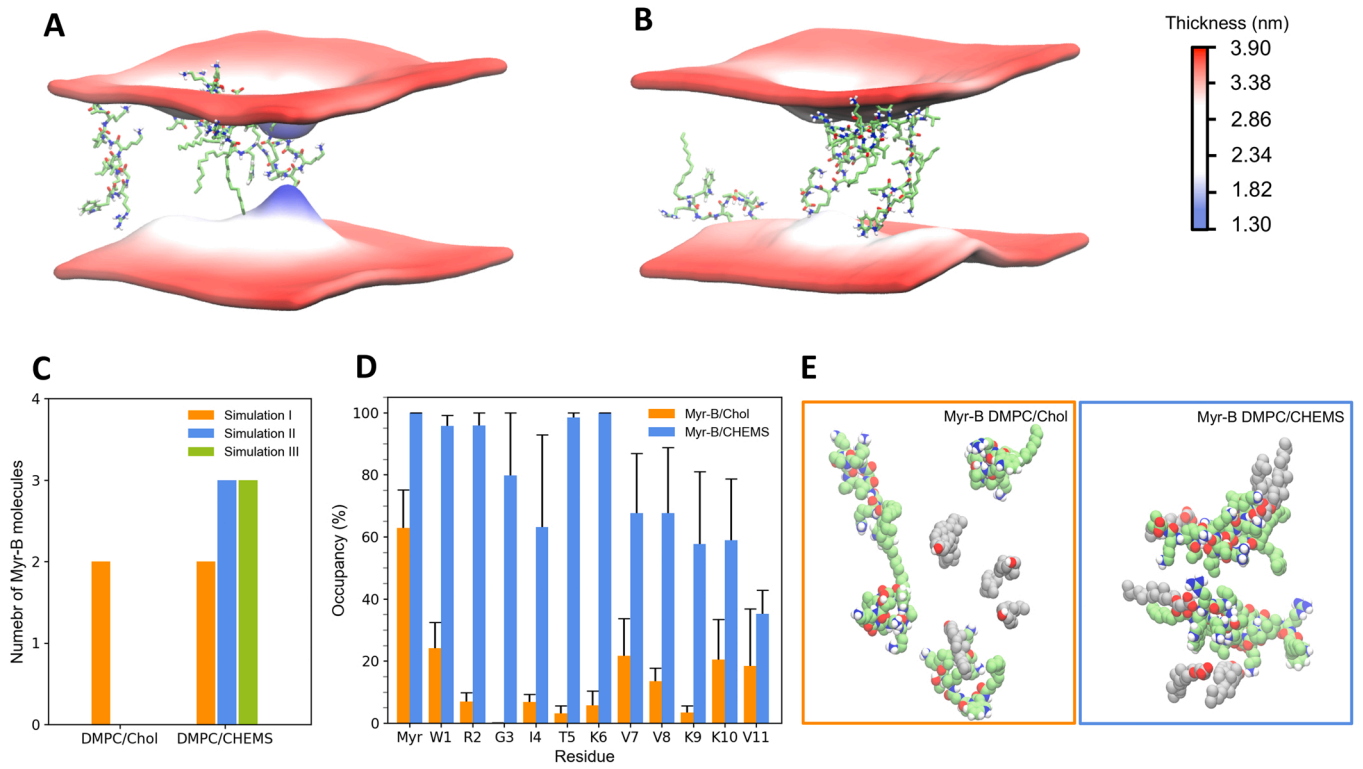

Fig. 3. Average local thickness of DMPC/Chol **A)** and DMPC/CHEMS **B)** in presence of Myr-B. The thickness increases as a blue-white-red colour gradient. Lipopeptides are represented in *licorice*. **C)** Number of Myr-B molecules with a sterol–peptide contact occupancy higher than 50% **D)** Histogram of sterol–peptide contact occupancy per Myr-B residue in DMPC/Chol (orange) and DMPC/CHEMS (blue). **E)** Representative snapshots of bilayer MD simulation in which is highlighted the sterol organization around Myr-B (lipid/peptide carbons in cyan; sterol carbons in grey).

Table 2
Minimum inhibitory concentration (MIC) in μg/mL (μM in parenthesis) of Myr-B and Myr-B loaded in liposomes against *C.albicans* and *C.tropicalis*.

Formulation	Tested isolates	
	C.albicans	*C.tropicalis*
Myr-B	50 (32.8)	12.5 (8.2)
Myr-B DMPC/Chol	3.13 (2.1)	3.13 (2.1)
Myr-B DMPC/Chol/CHEMS	1.94 (1.3)	3.88 (2.5)

not-encapsulated Myr-B had a good inhibition activity on *C.tropicalis*, and less efficacy on *C.albicans*. Liposomal encapsulation in both liposomal formulations resulted in a > 10-fold increase in inhibitory activity of Myr-B against *C. albicans* and in a 4-fold increase against *C. tropicalis* (Table 2). The empty liposomes tested at the same concentrations of Myr-B-loaded liposome did not exhibit antimicrobial activity.

2.3. LIVE and DEAD fluorescent assay

Fig. 4A and 4C (Figure S8 and FigureS9, [30]) shows representative images of fluorescent imaging sessions of *C.albicans* and *C.tropicalis* respectively, following treatment with Myr-B at MIC concentration, alone or encapsulated in liposomes. The rinsing step before performing the fluorescent dyeing excluded planktonic cells, focusing on adherent cells in an early biofilm stage [43]. Untreated *Candida* cells are reported as control. LIVE/DEAD fluorescent assay is composed of two fluorescent dyes: SYTO 9, highlighting alive cells with unaltered membrane integrity and emitting in the green; Propidium Iodide (PI), emitting in the red and entering only in membrane-damaged cells, replacing SYTO9. The green/red emission should be exclusive, but in this panel the treated *Candida* cells appear as a gradient between the two colors, creating a yellow composite. Treatment with free Myr-B and Myr-B-loaded formulations resulted in a marked reduction of biofilm biomass and a predominance of PI-positive signal in the merged images, indicative of extensive membrane disruption and cell death, whereas empty liposomes (DMPC/Chol and DMPC/Chol/CHEMS) and the untreated control displayed dense, largely SYTO9-positive biofilm networks consistent with retained cell viability. Fig. 4B and 4D (Figure S10, [30]) highlight that Myr-B, free and liposome-loaded, showed an important decrease in cell density compared to control, reducing drastically the presence of adherent yeast cells; a similar effect was already reported for Myr-B, used at a much higher concentration [23]. Liposomes alone seemed to promote yeast aggregation, resulting in a higher coverage of adherent cells, a phenomenon previously reported in the literature [44,45] but absent with Myr-B-loaded liposomes. These results, together with the MIC values (Table 2), confirm an enhanced *in-vitro* efficacy of Myr-B-loaded liposomes compared to free Myr-B.

2.4. Cytotoxicity against human cell line

To assess the effect of the formulations on cell viability, an ATP-Lite assay was performed using the primary human fibroblast line FB−789. Cell vitality was evaluated after 6 and 24 h of treatment with empty and Myr-B-loaded liposomes.

After 6 h Myr-B-loaded DMPC/Chol/CHEMS liposomes did not induce a reduction of cell viability (Fig. 5B): rather, a proliferative effect was evidenced at the highest tested peptide concentrations. On the contrary, empty DMPC/Chol/CHEMS liposomes evidenced a slight reduction of cell viability at low concentrations (about 15–20%). Both empty and Myr-B-loaded DMPC/Chol liposomes showed a low decrease

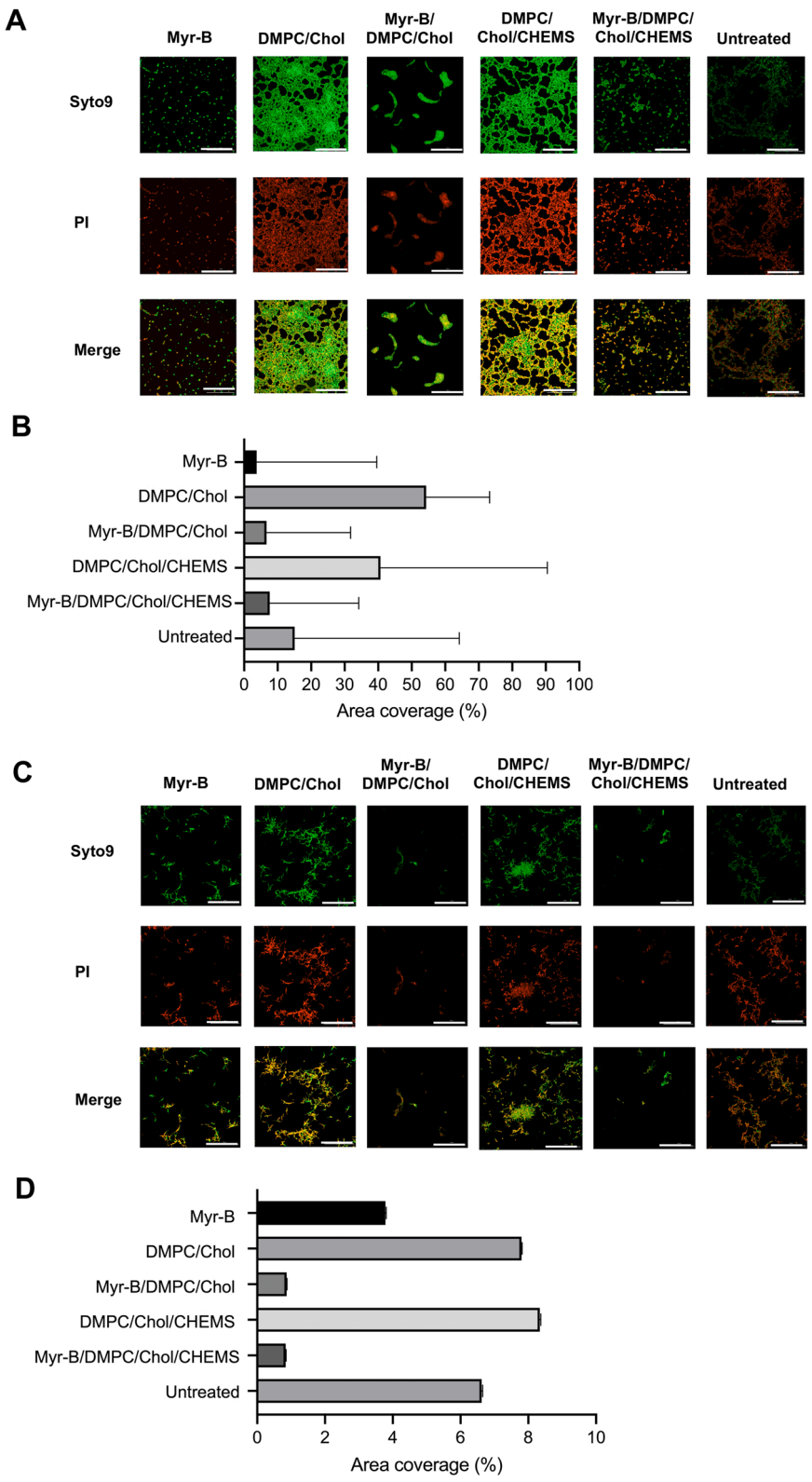

Fig. 4. LIVE/DEAD images of **A)** *C. albicans* and **C)** *C. tropicalis* treated with Myr-B, Myr-B-loaded -liposomes or untreated. Images were taken at 20x magnification, the scale bar placed in the right-bottom corresponds to 200 μm. Area coverage relative to total area of acquired fields of **B)** *C. albicans* and **D)** *C. tropicalis.*.

of cell viability at all tested concentrations (Fig. 5A).

The effect was slightly different after 24 h of treatment, (Fig. 5D), where about 85–90% of viability was observed for all the tested samples, except for 10 μM Myr-B for which a significant reduction of viability was observed. Myr-B-loaded DMPC/Chol liposomes did not affect cell viability (Fig. 5C), whereas empty liposomes caused slight cell death at all tested concentrations, with a significant difference from the control at 1.25, 2.5 and 5 μM.

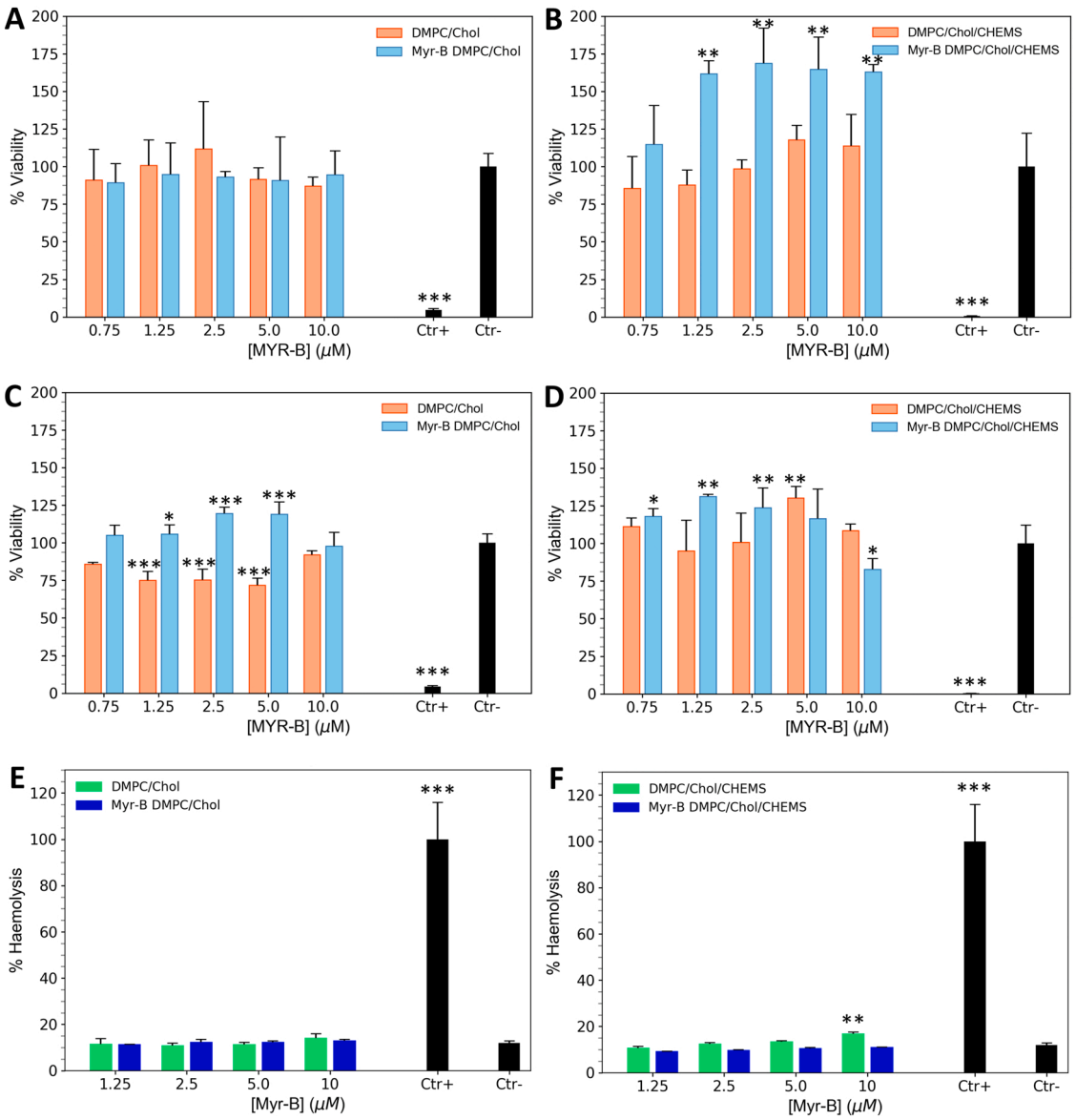

Fig. 5. A-D) Cell viability (%) vs. concentration of tested systems after 6 (**A**, **B**) and 24 h (**C**, **D**) of treatment. **E-F)** (Negative control: not treated cells; positive control: cells treated with 3% NaN_3). Haemolysis (%) vs. concentration of tested systems. (Negative control: not treated erythrocytes; positive control: erythrocytes treated with 2% Triton X). Empty liposomes were tested at the same lipid concentration of the loaded ones. Asterisks denote significance vs. negative control (black): *** = $p < 0.001$; ** = $p < 0.005$.

2.5. Haemolytic assay

A haemolytic assay against rabbit red blood cells was performed with DMPC/Chol and DMPC/Chol/CHEMS formulations both empty and loaded with Myr-B. As shown in Fig. 5E-F, the formulations were found to be not haemolytic at the tested concentrations. In fact, the haemolysis values of the tested samples were comparable to that of the negative control (erythrocytes incubated only with PBS buffer). Only the empty DMPC/Chol/CHEMS formulation (Fig. 5F) at the highest concentration showed a percentage of haemolysis with a significant difference from the control.

2.6. In-vivo toxicity evaluation on Galleria mellonella animal model

The *in-vivo* toxicity of Myr-B, liposomes, and Myr-B-loaded liposomes was assessed using the *Galleria mellonella* animal model [46]. Three days after administering the tested compounds at a concentration of 12.5 μg/mL (8.2 μM), only the DMPC/Chol/CHEMS group exhibited a low-rate toxicity in the larvae (Figure S11) [30]. All the other groups displayed a 100% vitality rate, suggesting promising potential for Myr-B-loaded liposomes, warranting further investigation into their *in-vivo* efficacy.

3. Conclusions

The development of liposome formulations for drug delivery requires a preliminary investigation aiming at selecting the optimal lipid composition together with the most suitable protocol of preparation in order to achieve liposomes with suitable dimension and PDI, high E.E., colloidal stability and drug retention over time. Although each drug constitutes a distinct case requiring specific investigation, certain general principles can still be applied to its study, while its investigation may yield additional general principles for future research.

In this work, we explored the inclusion of the antimicrobial lipopeptide Myr-B in DMPC-based liposomes with the aim of enhancing its antifungal activity while reducing its instability in biological

environment and tendency to aggregate.

A systematic investigation allowed to select two promising formulations (DMPC/Chol/Myr-B and DMPC/Chol/CHEMS/Myr-B) and the LC procedure resulted as the most effective. Molecular dynamics simulations highlighted that CHEMS markedly interacts with lipopeptide, affecting in turn peptide–lipid interactions, in particular bilayer compaction and organization, as well as peptide localization and release over time. Such evidence seems to corroborate with TEM investigation that reveals a peculiar *cartellate* type organization for liposomes including CHEMS.

Encapsulation significantly increased the antifungal potency of Myr-B, reducing MIC values more than ten-fold against *C.albicans* and four-fold against *C.tropicalis* for both liposome formulations. LIVE/DEAD imaging confirmed a substantial reduction in adherent fungal cells upon treatment with both Myr-B–loaded liposome formulations, highlighting their ability to impair early biofilm formation. It is worth noting that liposomes displayed low *in vitro* toxicity, minimal haemolytic activity, and favourable tolerability in *Galleria mellonella* larvae, supporting their suitability for further therapeutic development.

Notably, the moderate destabilization that Myr-B induces in the liposomal bilayer, as revealed by Molecular Dynamic simulations could be functionally advantageous because it facilitates the liberation of Myr-B at the site of action and likely contribute to the enhanced antifungal activity of Myr-B liposomes.

Overall, our findings enabled the development of two Myr-B-loaded liposomal formulations with strong antifungal activity and low toxicity, making them promising candidates for further preclinical evaluation as treatments for invasive fungal infections. Noteworthy, the chemico-physics investigation provided here, beyond elucidating the key features of the lipid bilayer of Myr-B-loaded liposomal formulations, lay the groundwork for future investigation into incorporating other AMPs into liposomes.

4. Experimental section

A detailed version of the material and methods section is available in the Zenodo repository [30].

4.1. Material

Dimyristoyl-*sn*-glycero−3-phosphocholine (DMPC, purity >99%) was purchased from Avanti Polar Lipids (Alabaster, AL) and was used without further purification. Cholesterol (Chol), cholesteryl hemisuccinate (CHEMS) and Sephadex G−50 fine resin were purchased from Merck. The antimicrobial peptide Myr-B (Myr-WRGITKVVKKV) was purchased from CASLO ApS, c/o Technical University of Denmark, with a purity > 98%. Organic solvents were purchased from VWR. All aqueous solutions were prepared using ultrapure MilliQ water produced by a Millipore DirectQ3 apparatus. Phosphate buffer solution (10 mM) was prepared by dissolving sodium dihydrogenphosphate and disodium hydrogenphosphate dodecahydrate in water and adjusting the pH to 7.4 with a sodium hydroxide solution.

4.2. Preparation and purification of empty and Myr-B-loaded liposomes

Liposomes were prepared according to two methods: the thin lipid film hydration method coupled with the freeze-thaw protocol and extrusion [47] (TFH), and the lipid cake method [37] (LC). Size exclusion chromatography was used to remove the Myr-B peptide not included into the liposomes. [48].

4.3. Size and ζ-potential measurements

Liposome suspensions were analysed by Dynamic Light Scattering (DLS) and Dielectrophoretic Light Scattering (DELS) to assess their mean diameter, polydispersity index (PDI), and ζ-potential. A Malvern Nano-ZetaSizer apparatus, operating in backscattering (173 °) and equipped with a 5 mW HeNe laser (λ = 632.8 nm), a thermostatted sample holder and a digital logarithmic correlator was used to perform both DLS and DELS measurements. Both size and ζ-potential were measured at 25 °C.

4.4. Determination of Myr-B entrapment efficiency (EE%)

The concentration of Myr-B entrapped in liposomes was evaluated by UV-Vis spectroscopy measurements. The calibration curve was built by using tryptophan (Trp) solutions of known concentration.

Liposomes were broken up before the measurement by 1:1 (v/v) water isopropanol solution. Myr-B concentration was calculated by the absorbance at 280 nm, and the EE % was evaluated by the following equation:

$$EE\% = \frac{[Myr-B]_{ae}}{[Myr-B]_0} \times 100$$

where $[Myr-B]_0$ and $[Myr-B]_{ae}$ indicate the concentration of lipopeptide at the beginning and at the end of the preparation, respectively.

4.5. Morphological characterization of liposomes by transmission electron microscopy (TEM)

The morphology of liposomes was investigated by TEM coupled with negative staining protocol (JEOL 1200 EX II). Micrographs were acquired by the Olympus SIS VELETA CCD camera; the average dimension was obtained using the software iTEM (Olympus).

4.6. Molecular dynamics simulations

The molecular systems were built by using minimum bias approach [39,40] starting with a random orientation of both Myr-B and lipid molecules in the simulation box. The initial structure of Myr-B was obtained after 300 ns of MD simulation in water. The composition of the simulated systems is reported in Table S2. Each system was energy minimized and 100 ps of MD simulation, with positional restrains (force constant of 1000 kJ mol^{-1} nm^{-2}) on the backbone of peptides, were performed at 298 K with an isotropic pressure coupling at 1 bar. Finally, 2 μs of unrestrained MD simulation was performed at 298 K and 1 atm with an anisotropic control of pressure. For each molecular system three independent MD simulation were performed.

The peptides were modelled by using GROMOS G54a8 [49,50] force field in conjunction with the GROMOS G54a8-v1 [51] for the lipids DMPC. The parameters for sterol molecules were taken from O'Mara et al. [52] The GROMOS G54a8-v1 bonding and non-bonding parameters of the glutamic acid side chain were used to model the hemisuccinyl moiety of CHEMS. The GROMACS topology of cholesterol and CHEMS are available in the Zenodo repository [30].

The Simple Point Charge (SPC) [53] model was used for water.

All bonds were constrained using the P-LINCS algorithm [54] whereas the geometry of water molecules was fixed with the SETTLE algorithm [55]. The temperature of the simulated systems was controlled by coupling the peptides, lipids, water and ions to an external bath at 298 K by using the velocity-rescale [56] thermostat with a coupling constant of 0.1 ps. The pressure was kept constant at 1 bar by using the Berendsen barostat [57] and in the last 1 μs of simulation the Parinello-Rahman barostat [58] (P = 1 bar, τ_P = 4 ps) was used. The analysis of the trajectories was performed on the last 1 μs of MD simulations.

4.7. Minimum inhibitory concentration (MIC) determination

Both tested strains were derived from positive blood cultures and identified via matrix assisted laser desorption ionization – time of flight mass spectrometry (Bruker, Massachusetts, U.S.A.). The MIC

concentrations of Myr-B free and liposome-loaded were determined by microbroth dilution method, in a 96-well u-bottom plate Falcon (Corning incorporated, New York, U.S.A.) following EUCAST-AFST (European Society for Clinical Microbiology and Infectious Diseases – AntiFungal Susceptibility Testing) guidelines [59].

4.8. Live and dead fluorescent assay

The assay was performed by using LIVE/DEAD™ BacLight™ Bacterial Viability Kit (Termofisher scientific; Waltham, Massachusetts, USA), following manufacturer instructions. The fluorescent imaging was conducted by Cytation 5 Cell Imaging Multi-Mode Reader, with an excitation/emission wavelengths of 469/525 nm for SYTO9 and 586/647 nm for Propidium Iodide (PI).

4.9. Image quantitative analysis

Area coverage was calculated through Fiji ImageJ software (Version 1.53c) using the auto-threshold tool. The percentage values refer to part of the field, measured in pixels, actually covered with yeast cells (both live and dead) compared to the whole area of the image.

4.10. In vivo cytotoxicity on galleria mellonella

The *in vivo* cytotoxicity of Myr-B free or liposome-loaded was assessed on the animal model of *G. mellonella* larvae. Treatments and control groups were formed by twenty larvae each. After the treatments, larvae were incubated at 33 °C in aerobic conditions. The viability of larvae was visually evaluated every 24 h for 72 h. Lack of mobility after stimulation and melanization were considered as death indicators according to Loh et al. criteria [46]. Cocoon formation was excluded as criteria because the phenomenon was not observed in the 3 days of observational period.

4.11. Cytotoxicity assay against human cell line

The cytotoxicity of Myr-B free or liposome-loaded was determined with the ATPLite Luminescence Assay using a primary human fibroblast cell line (FB789) [23].

The percentage of cell viability was determined as follows:

$$\%Cells\ viability = \frac{RLU_{Test\ group}}{RLU_{Negative\ control}} \times 100$$

where RLU is the unit of relative light measured by the instrument.

4.12. Haemolytic assay against rabbit erythrocytes

The haemolytic activity was evaluated by adding increasing concentrations of Myr-B (from 1.25 to 10 μM) encapsulated in the different liposomes and the corresponding quantities of empty liposomes to rabbit erythrocytes (Rockland) previously purified and maintained in Alsever's solution. After removing Alsever's solution by centrifugation, the erythrocytes were washed and resuspended in PBS to the appropriate dilution. Erythrocytes were incubated only with PBS buffer as a negative control and in the presence of Triton X−100 at 2% (v/v) as a positive control.

The haemolysis percentage was calculated as follows:

$$\%Hemolysis = \frac{(A_{Test\ group})}{(A_{Positive\ control})} \times 100$$

4.13. Statistical analysis

The results of the cytotoxic and haemolytic experiments are expressed as the mean ± SD and the differences from the controls have been considered significant if $p < 0.05$ using a statistical analysis performed by the one-way ANOVA followed by the Bonferroni test (*** = $p < 0.001$; ** = $p < 0.005$. *$p < 0.01$). Microbiological testing was performed in triplicate and are expressed, where appropriate, as mean ± SD.

ASSOCIATED CONTENT

The supporting information file is available in Zenodo [30] and contains: a detailed version of material and methods section; preliminary experiments to define the final Myr-B/liposome composition; the release assay of Myr-B from liposomes; the plots of colloidal stability of liposomes in PB and in the presence of FCS 10%; the plots of the ζ-potential over time of liposomes in PB; lipid bilayers and Myr-B/lipid bilayers systems studied by MD simulations; snapshots of self-assembly of Myr-B and the mixture of DMPC CHEMS in water; Mass density profiles across the lipid bilayer; occupancy of the contacts between Myr-B and Chol and CHEMS molecules, full-pages images of LIVE/DEAD assay, plot of *in-vivo* toxicity assessment on *Galleria mellonella* larvae.

CRediT authorship contribution statement

Federica Massaro: Writing – review & editing, Writing – original draft, Visualization, Investigation, Formal analysis. **Fernando Porcelli:** Writing – review & editing, Supervision, Resources, Methodology, Funding acquisition, Conceptualization. **Fabiana Pandolfi:** Writing – review & editing, Methodology, Investigation, Formal analysis. **Cecilia Bombelli:** Writing – review & editing, Writing – original draft, Visualization, Validation, Resources, Methodology, Data curation, Conceptualization. **Federica Toma:** Writing – review & editing, Writing – original draft, Visualization, Investigation, Formal analysis. **Antonia Volpe:** Writing – review & editing, Investigation. **Francesca Ceccacci:** Writing – review & editing, Resources, Project administration, Funding acquisition, Conceptualization. **Stefano Borocci:** Writing – review & editing, Writing – original draft, Visualization, Validation, Resources, Methodology, Investigation, Funding acquisition, Data curation, Conceptualization. **Mariangela Clemente:** Writing – review & editing, Validation, Investigation, Data curation. **Damiano Squitieri:** Writing – review & editing, Writing – original draft, Visualization, Investigation, Formal analysis. **Francesca Bugli:** Writing – review & editing, Writing – original draft, Validation, Resources, Methodology, Funding acquisition, Formal analysis, Data curation. **Francesco Buonocore:** Writing – review & editing, Writing – original draft, Supervision, Resources, Project administration, Funding acquisition, Conceptualization. **Anna Rita Taddei:** Writing – review & editing, Investigation.

Declaration of Generative AI and AI-assisted technologies in the writing process

During the preparation of this work the authors used Copilot to check english language for some sentences. After using this tool, the authors reviewed and edited the content as needed and take full responsibility for the content of the published article.

Funding

F.Bug. and C.B. acknowledge funding from the project "One Health Basic and Translational Research Actions addressing Unmet Needs on Emerging Infectious Diseases-INFACT"-PNRR NextGenerationEU.

F.B., F.C., F.P., S.B., F.Bug. acknowledge funding from PRIN project 2022 "Fish-inspired antimicrobial peptide delivered by specific nanosystems to fight ESKAPE bacteria: a powerful weapon against antibiotic resistance" -FIDEANT (project n. 2022FKLKSY) funded by the European Union – Next Generation EU.

S.B. acknowledges funding from "Project ECS 0000024 Rome Technopole, – CUP B83C22002820006, NRP Mission 4 Component 2 Investment 1.5, Funded by the European Union – NextGenerationEU".

Declaration of Competing Interest

The authors declare the following financial interests/personal relationships which may be considered as potential competing interests: Stefano Borocci, Francesca Ceccacci, Fernando Porcelli, Francesco Buoncore and Francesca Bugli reports financial support was provided by Italian Ministry of University and Research. Cecilia Bombelli, Francesca Bugli reports financial support was provided by European Union-PNRR NextGenerationEU. Stefano Borocci reports financial support was provided by European Union-PNRR NextGenerationEU. If there are other authors, they declare that they have no known competing financial interests or personal relationships that could have appeared to influence the work reported in this paper.

Acknowledgment

S.B. thanks the University of Tuscia for the allowed use of the DIBAF Cluster HPC Infrastructure where all the molecular dynamics simulations were carried out.

Data availability

Data will be made available on request.

References

[1] M. Naghavi, S.E. Vollset, K.S. Ikuta, L.R. Swetschinski, A.P. Gray, E.E. Wool, G. Robles Aguilar, T. Mestrovic, G. Smith, C. Han, R.L. Hsu, J. Chalek, D.T. Araki, E. Chung, C. Raggi, A. Gershberg Hayoon, N. Davis Weaver, P.A. Lindstedt, A. E. Smith, U. Altay, N.V. Bhattacharjee, K. Giannakis, F. Fell, B. McManigal, N. Ekapirat, J.A. Mendes, T. Runghien, O. Srimokla, A. Abdelkader, S. Abd-Elsalam, R.G. Aboagye, H. Abolhassani, H. Abualruz, U. Abubakar, H. J. Abukhadijah, S. Aburuz, A. Abu-Zaid, S. Achalapong, I.Y. Addo, V. Adekanmbi, T.E. Adeyeoluwa, Q.E.S. Adnani, L.A. Adzigbli, M.S. Afzal, S. Afzal, A. Agodi, A. J. Ahlstrom, A. Ahmad, S. Ahmad, T. Ahmad, A. Ahmadi, A. Ahmed, H. Ahmed, I. Ahmed, M. Ahmed, S. Ahmed, S.A. Ahmed, M.A. Akkaif, S. Al Awaidy, Y. Al Thaher, S.O. Alalalmeh, M.T. AlBataineh, W.A. Aldhaleei, A.A.S. Al-Gheethi, N. B. Alhaji, A. Ali, L. Ali, S.S. Ali, W. Ali, K. Allel, S. Al-Marwani, A. Alrawashdeh, A. Altaf, A.B. Al-Tammemi, J.A. Al-Tawfiq, K.H. Alzoubi, W.A. Al-Zyoud, B. Amos, J.H. Amuasi, R. Ancuceanu, J.R. Andrews, A. Anil, I.A. Anuoluwa, S. Anvari, A. E. Anyasodor, G.L.C. Apostol, J. Arabloo, M. Arafat, A.Y. Aravkin, D. Areda, A. Aremu, A.A. Artamonov, E.A. Ashley, M.O. Asika, S.S. Athari, M.M.W. Atout, T. Awoke, S. Azadnajafabad, J.M. Azam, S. Aziz, A.Y. Azzam, M. Babaei, F. X. Babin, M. Badar, A.A. Baig, M. Bajcetic, S. Baker, M. Bardhan, H.J. Barqawi, Z. Basharat, A. Basiru, M. Bastard, S. Basu, N.S. Bayleyegn, M.A. Belete, O.O. Bello, A. Beloukas, J.A. Berkley, A.S. Bhagavathula, S. Bhaskar, S.S. Bhuyan, J.A. Bielicki, N.I. Briko, C.S. Brown, A.J. Browne, D. Buonsenso, Y. Bustanji, C.G. Carvalheiro, C. A. Castañeda-Orjuela, M. Cenderadewi, J. Chadwick, S. Chakraborty, R. M. Chandika, S. Chandy, V. Chansamouth, V.K. Chattu, A.A. Chaudhary, P. R. Ching, H. Chopra, F.R. Chowdhury, D.T. Chu, M. Chutiyami, N. Cruz-Martins, A. G. da Silva, O. Dadras, X. Dai, S.D. Darcho, S. Das, F.P. De La Hoz, D.M. Dekker, K. Dhama, D. Diaz, B.F.R. Dickson, S.G. Djorie, M. Dodangeh, S. Dohare, K. G. Dokova, O.P. Doshi, R.K. Dowou, H.L. Dsouza, S.J. Dunachie, A.M. Dziedzic, T. Eckmanns, A. Ed-Dra, A. Eftekharimehrabad, T.C. Ekundayo, I. El Sayed, M. Elhadi, W. El-Huneidi, C. Elias, S.J. Ellis, R. Elsheikh, I. Elsohaby, C. Eltaha, B. Eshrati, M. Eslami, D.W. Eyre, A.O. Fadaka, A.F. Fagbamigbe, A. Fahim, A. Fakhri-Demeshghieh, F.O. Fasina, M.M. Fasina, A. Fatehizadeh, N.A. Feasey, A. Feizkhah, G. Fekadu, F. Fischer, I. Fitriana, K.M. Forrest, C. Fortuna Rodrigues, J.E. Fuller, M.A. Gadanya, M. Gajdács, A.P. Gandhi, E.E. Garcia-Gallo, D.O. Garrett, R.K. Gautam, M.W. Gebregergis, M. Gebrehiwot, T.G. Gebremeskel, C. Geffers, L. Georgalis, R.M. Ghazy, M. Golechha, D. Golinelli, M. Gordon, S. Gulati, R. Das Gupta, S. Gupta, V.K. Gupta, A.D. Habteyohannes, S. Haller, H. Harapan, M. L. Harrison, A.I. Hasaballah, I. Hasan, R.S. Hasan, H. Hasani, A.H. Haselbeck, M. S. Hasnain, I.I. Hassan, S. Hassan, M.S. Hassan Zadeh Tabatabaei, K. Hayat, J. He, O.E. Hegazi, M. Heidari, K. Hezam, R. Holla, M. Holm, H. Hopkins, M.M. Hossain, M. Hosseinzadeh, S. Hostiuc, N.R. Hussein, L.D. Huy, E.D. Ibáñez-Prada, A. Ikiroma, I.M. Ilic, S.M.S. Islam, F. Ismail, N.E. Ismail, C.D. Iwu, C.J. Iwu-Jaja, A. Jafarzadeh, F. Jaiteh, R. Jalilzadeh Yengejeh, R.D.G. Jamora, J. Javidnia, T. Jawaid, A.W.J. Jenney, H.J. Jeon, M. Jokar, N. Jomehzadeh, T. Joo, N. Joseph, Z. Kamal, K.K. Kanmodi, R.S. Kantar, J.A. Kapisi, I.M. Karaye, Y.S. Khader, H. Khajuria, N. Khalid, F. Khamesipour, A. Khan, M.J. Khan, M.T. Khan, V. Khanal, F.F. Khidri, J. Khubchandani, S. Khusuwan, M.S. Kim, A. Kisa, V.A. Korshunov, F. Krapp, R. Krumkamp, M. Kuddus, M. Kulimbet, D. Kumar, E.A.P. Kumaran, A. Kuttikkattu, H.H. Kyu, I. Landires, B.K. Lawal, T.T.T. Le, I.M. Lederer, M. Lee, S. W. Lee, A. Lepape, T.L. Lerango, V.S. Ligade, C. Lim, S.S. Lim, L.W. Limenh, C. Liu, X. Liu, X. Liu, M.J. Loftus, H.I.M. Amin, K.L. Maass, S.B. Maharaj, M.A. Mahmoud, P. Maikanti-Charalampous, O.M. Makram, K. Malhotra, A.A. Malik, G. D. Mandilara, F. Marks, B.A. Martinez-Guerra, M. Martorell, H. Masoumi-Asl, A. G. Mathioudakis, J. May, T.A. McHugh, J. Meiring, H.N. Meles, A. Melese, E. B. Melese, G. Minervini, N.S. Mohamed, S. Mohammed, S. Mohan, A.H. Mokdad, L. Monasta, A.A. Moodi Ghalibaf, C.E. Moore, Y. Moradi, E. Mossialos, V. Mougin, G.D. Mukoro, F. Mulita, B. Muller-Pebody, E. Murillo-Zamora, S. Musa, P. Musicha, L.A. Musila, S. Muthupandian, A.J. Nagarajan, P. Naghavi, F. Nainu, T.S. Nair, H.H. R. Najmuldeen, Z.S. Natto, J. Nauman, B.P. Nayak, G.T. Nchanji, P. Ndishimye, I. Negoi, R.I. Negoi, S.A. Nejadghaderi, Q.A.P. Nguyen, E.A. Noman, D. C. Nwakanma, S. O'Brien, T.J. Ochoa, I.A. Odetokun, O.A. Ogundijo, T.R. Ojo-Akosile, S.R. Okeke, O.C. Okonji, A.T. Olagunju, A. Olivas-Martinez, A. A. Olorukooba, P. Olwoch, K.I. Onyedibe, E. Ortiz-Brizuela, O. Osuolale, P. Ounchanum, O.T. Oyeyemi, P.A.M. Padukudru, J.L. Paredes, R.R. Parikh, J. Patel, S. Patil, S. Pawar, A.Y. Peleg, P. Peprah, J. Perdigão, C. Perrone, I.R. Petcu, K. Phommasone, Z.Z. Piracha, D. Poddighe, A.J. Pollard, R. Poluru, A. Ponce-De-Leon, J. Puvvula, F.N. Qamar, N.H. Qasim, C.D. Rafai, P. Raghav, L. Rahbarnia, F. Rahim, V. Rahimi-Movaghar, M. Rahman, M.A. Rahman, H. Ramadan, S. K. Ramasamy, P.S. Ramesh, P.W. Ramteke, R.K. Rana, U. Rani, M.M. Rashidi, D. Rathish, S. Rattanavong, S. Rawaf, E.M.M. Redwan, L.F. Reyes, T. Roberts, J. V. Robotham, V.D. Rosenthal, A.G. Ross, N. Roy, K.E. Rudd, C.J. Sabet, B.A. Saddik, M.R. Saeb, U. Saeed, S. Saeedi Moghaddam, W. Saengchan, M. Safaei, A. Saghazadeh, N. Saheb Sharif-Askari, A. Sahebkar, S.S. Sahoo, M. Sahu, M. Saki, N. Salam, Z. Saleem, M.A. Saleh, Y.L. Samodra, A.M. Samy, A. Saravanan, M. Satpathy, A.E. Schumacher, M. Sedighi, S. Seekaew, M. Shafie, P.A. Shah, S. Shahid, M.J. Shahwan, S. Shakoor, N. Shalev, M.A. Shamim, M. A. Shamshirgaran, A. Shamsi, A. Sharifan, R.P. Shastry, M. Shetty, A. Shittu, S. Shrestha, E.E. Siddig, T. Sideroglou, J. Sifuentes-Osornio, L.M.L.R. Silva, E.A. F. Simões, A.J.H. Simpson, A. Singh, S. Singh, R. Sinto, S.S.M. Soliman, S. Soraneh, N. Stoesser, T.Z. Stoeva, C.K. Swain, L. Szarpak, T.Y. Sree Sudha, S. Tabatabai, C. Tabche, Z.M.A. Taha, K.K. Tan, N. Tasak, N.Y. Tat, A. Thaiprakong, P. Thangaraju, C.C. Tigoi, K. Tiwari, M.R. Tovani-Palone, T.H. Tran, M. Tumurkhuu, P. Turner, A.J. Udoakang, A. Udoh, N. Ullah, S. Ullah, A. G. Vaithinathan, M. Valenti, T. Vos, H.T.L. Vu, Y. Waheed, A.S. Walker, J. L. Walson, T. Wangrangsimakul, K.G. Weerakoon, H.F.L. Wertheim, P.C. M. Williams, A.A. Wolde, T.M. Wozniak, F. Wu, Z. Wu, M.K.K. Yadav, S. Yaghoubi, Z.S. Yahaya, A. Yarahmadi, S. Yezli, Y.E. Yismaw, D.K. Yon, C.W. Yuan, H. Yusuf, F. Zakham, G. Zamagni, H. Zhang, Z.J. Zhang, M. Zielińska, A. Zumla, S.H. H. Zyoud, S.H. Zyoud, S.I. Hay, A. Stergachis, B. Sartorius, B.S. Cooper, C. Dolecek, C.J.L. Murray, Global burden of bacterial antimicrobial resistance 1990–2021: a systematic analysis with forecasts to 2050, Lancet 404 (2024) 1199–1226, https://doi.org/10.1016/S0140-6736(24)01867-1.

[2] K. Browne, S. Chakraborty, R. Chen, M.D.P. Willcox, D.S. Black, W.R. Walsh, N. Kumar, A new era of antibiotics: the clinical potential of antimicrobial peptides, Int. J. Mol. Sci. 21 (2020) 7047–7070, https://doi.org/10.3390/ijms21197047.

[3] S. Nagaraj, S. Manivannan, S. Narayan, Potent antifungal agents and use of nanocarriers to improve delivery to the infected site: a systematic review, J. Basic. Microbiol. 61 (2021) 849–873, https://doi.org/10.1002/jobm.202100204.

[4] M. Mahlapuu, J. Håkansson, L. Ringstad, C. Björn, Antimicrobial peptides: an emerging category of therapeutic agents, Front. Cell. Infect. Microbiol. 6 (2016) 194–206, https://doi.org/10.3389/fcimb.2016.00194.

[5] L. Bardet, S. Le Page, T. Leangapichart, J.M. Rolain, LBJMR medium: a new polyvalent culture medium for isolating and selecting vancomycin and colistin-resistant bacteria, BMC Microbiol. 17 (2017) 220–230, https://doi.org/10.1186/s12866-017-1128-x.

[6] R. Fani, A.H. Mondal, K. Khare, P. Saxena, P. Debnath, K. Mukhopadhyay, D. Yadav, A Review on Colistin Resistance: An Antibiotic of Last Resort, Microorganisms 12 (2024) 772–780, https://doi.org/10.3390/microorganisms12040772.

[7] Z. Li, Z. Cui, D. Xie, F. Zou, C. Zhu, Unveiling the hidden risk of caspofungin: insights from three adverse event reporting systems and network pharmacology integration, Front. Pharmacol. 16 (2025), https://doi.org/10.3389/fphar.2025.1632488, 1632488–1632508.

[8] CDC, Antibiotic resistance threats in the United States, 2019. Cent. Dis. Control Prev., U.S. Department of Health and Human Services, Atlanta, GA, 2019.

[9] A.C. Spencer, K.R. Brubaker, S. Garneau-Tsodikova, Systemic fungal infections: A pharmacist/researcher perspective, Fungal Biol. Rev. 44 (2023) 100293, https://doi.org/10.1016/j.fbr.2022.11.001.

[10] R. Maji, S. Chowdhury, K. Kar, K. Mazumder, Current Strategies for Addressing Antibiotic Resistance: A Comprehensive Review, J. Bio-X Res. 8 (2025) 2577–3585, https://doi.org/10.34133/jbioxresearch.0040.

[11] H. Gong, M.A. Sani, X. Hu, K. Fa, J.W. Hart, M. Liao, P. Hollowell, J. Carter, L. A. Clifton, M. Campana, P. Li, S.M. King, J.R.P. Webster, A. Maestro, S. Zhu, F. Separovic, T.A. Waigh, H. Xu, A.J. McBain, J.R. Lu, How do Self-Assembling Antimicrobial Lipopeptides Kill Bacteria? ACS Appl. Mater. Interfaces 12 (2020) 55675–55687, https://doi.org/10.1021/acsami.0c17222.

[12] A. Malina, Y. Shai, Conjugation of fatty acids with different lengths modulates the antibacterial and antifungal activity of a cationic biologically inactive peptide, Biochem. J. 390 (2005) 695–702, https://doi.org/10.1042/BJ20050520.

[13] M.C. Teixeira, C. Carbone, M.C. Sousa, M. Espina, M.L. Garcia, E. Sanchez-Lopez, E. B. Souto, Nanomedicines for the delivery of antimicrobial peptides (Amps), Nanomaterials 10 (2020) 1–23, https://doi.org/10.3390/nano10030560.

[14] Á. Martin-Serrano, R. Gómez, P. Ortega, F.J.D. La Mata, Nanosystems as vehicles for the delivery of antimicrobial peptides (Amps), Pharmaceutics 11 (2019) 448–473, https://doi.org/10.3390/pharmaceutics11090448.

[15] Z. Drulis-Kawa, A. Dorotkiewicz-Jach, Liposomes as delivery systems for antibiotics, Int. J. Pharm. 387 (2010) 187–198, https://doi.org/10.1016/j.ijpharm.2009.11.033.

[16] M. Alhariri, A. Azghani, A. Omri, Liposomal antibiotics for the treatment of infectious diseases, Expert. Opin. Drug. Deliv. 10 (2013) 1515–1532, https://doi.org/10.1517/17425247.2013.822860.
[17] S. Hallaj-Nezhadi, M. Hassan, Nanoliposome-based antibacterial drug delivery, Drug. Deliv. 22 (2015) 581–589, https://doi.org/10.3109/10717544.2013.863409.
[18] M. Ferreira, M. Ogren, J.N.R. Dias, M. Silva, S. Gil, L. Tavares, F. Aires-Da-silva, M. M. Gaspar, S.I. Aguiar, Liposomes as antibiotic delivery systems: A promising nanotechnological strategy against antimicrobial resistance, Molecules 26 (2021) 2047–2073, https://doi.org/10.3390/molecules26072047.
[19] M. Faya, H.A. Hazzah, C.A. Omolo, N. Agrawal, R. Maji, P. Walvekar, C. Mocktar, B. Nkambule, S. Rambharose, F. Albericio, B.G. de la Torre, T. Govender, Novel formulation of antimicrobial peptides enhances antimicrobial activity against methicillin-resistant Staphylococcus aureus (MRSA), Amino Acids 52 (2020) 1439–1457, https://doi.org/10.1007/s00726-020-02903-7.
[20] C. Pu, W. Tang, The antibacterial and antibiofilm efficacies of a liposomal peptide originating from rice bran protein against: Listeria monocytogenes, Food Funct. 8 (2017) 4159–4169, https://doi.org/10.1039/c7fo00994a.
[21] N. Vera-González, C.M. Bailey-Hytholt, L. Langlois, F. de Camargo Ribeiro, E.L. de Souza Santos, J.C. Junqueira, A. Shukla, Anidulafungin liposome nanoparticles exhibit antifungal activity against planktonic and biofilm Candida albicans, J. Biomed. Mater. Res. - Part. A 108 (2020) 2263–2276, https://doi.org/10.1002/jbm.a.36984.
[22] C. Olivieri, F. Bugli, G. Menchinelli, G. Veglia, F. Buonocore, G. Scapigliati, V. Stocchi, F. Ceccacci, M. Papi, M. Sanguinetti, F. Porcelli, Design and characterization of chionodracine-derived antimicrobial peptides with enhanced activity against drug-resistant human pathogens, RSC Adv. 8 (2018) 41331–41346, https://doi.org/10.1039/C8RA08065H.
[23] Francesca Bugli, Federica Massaro, Francesco Buonocore, Paolo Roberto Saraceni, Stefano Borocci, Francesca Ceccacci, Cecilia Bombelli, Maura Di Vito, Rosalba Marchitiello, Melinda Mariotti, Riccardo Torelli, Maurizio Sanguinetti, Fernando Porcelli, Design and Characterization of Myristoylated and Non-Myristoylated Peptides Effective against Candida spp. Clinical Isolates, Int. J. Mol. Sci. 23 (2022) 2164–2186, https://doi.org/10.3390/ijms23042164.
[24] D.W. Denning, Global incidence and mortality of severe fungal disease, Lancet Infect. Dis. 24 (2024) e428–e438, https://doi.org/10.1016/S1473-3099(23)00692-8.
[25] P.G. Pappas, C.A. Kauffman, D.R. Andes, C.J. Clancy, K.A. Marr, L. Ostrosky-Zeichner, A.C. Reboli, M.G. Schuster, J.A. Vazquez, T.J. Walsh, T.E. Zaoutis, J. D. Sobel, Clinical Practice Guideline for the Management of Candidiasis: 2016 Update by the Infectious Diseases Society of America, Clin. Infect. Dis. 62 (2015) e1–50, https://doi.org/10.1093/cid/civ933.
[26] B.J. Kullberg, M.C. Arendrup, Invasive Candidiasis, N. Engl. J. Med. 373 (2015) 1445–1456, https://doi.org/10.1056/NEJMra1315399.
[27] C.M. de Souza, M.M. dos Santos, L. Furlaneto-Maia, M.C. Furlaneto, Adhesion and biofilm formation by the opportunistic pathogen Candida tropicalis: What do we know? Can. J. Microbiol. 69 (2023) 206–218, https://doi.org/10.1139/cjm-2022-0195.
[28] M.B. Atiencia-Carrera, F.S. Cabezas-Mera, E. Tejera, A. Machado, Prevalence of biofilms in Candida spp. bloodstream infections: A meta-analysis, PLoS. One 17 (2022) e0263522–e0263545, https://doi.org/10.1371/journal.pone.0263522.
[29] M. Tumbarello, B. Posteraro, E.M. Trecarichi, B. Fiori, M. Rossi, R. Porta, K.D. G. Donati, M. La Sorda, T. Spanu, G. Fadda, R. Cauda, M. Sanguinetti, Biofilm production by Candida species and inadequate antifungal therapy as predictors of mortality for patients with candidemia, J. Clin. Microbiol. 45 (2007) 1843–1850, https://doi.org/10.1128/JCM.00131-07.
[30] F. Toma, A. Volpe, F. Pandolfi, F. Massaro, F. Porcelli, F. Buonocore, A.R. Taddei, D. Squitieri, F. Bugli, F. Ceccacci, S. Borocci, M. Clemente, C. Bombelli, Additional data of the study about Myr-B loaded-liposomes, Zenodo (2026), https://doi.org/10.5281/zenodo.19112376.
[31] L.M. Were, B.D. Bruce, P.M. Davidson, J. Weiss, Size, Stability, and Entrapment Efficiency of Phospholipid Nanocapsules Containing Polypeptide Antimicrobials, J. Agric. Food Chem. 51 (2003) 8073–8079, https://doi.org/10.1021/jf0348368.
[32] D. Nicolosi, S. Cupri, C. Genovese, G. Tempera, R. Mattina, R. Pignatello, Nanotechnology approaches for antibacterial drug delivery: Preparation and microbiological evaluation of fusogenic liposomes carrying fusidic acid, Int. J. Antimicrob. Agents 45 (2015) 622–626, https://doi.org/10.1016/j.ijantimicag.2015.01.016.
[33] C.B. Garcia, D. Shi, T.J. Webster, Tat-functionalized liposomes for the treatment of meningitis: An in vitro study, Int. J. Nanomed. 12 (2017), https://doi.org/10.2147/IJN.S130125.
[34] I.M. Hafez, S. Ansell, P.R. Cullis, Tunable pH-Sensitive Liposomes Composed of Mixtures of Cationic and Anionic Lipids, Biophys. J. 79 (2000) 1438–1446, https://doi.org/10.1016/S0006-3495(00)76395-8.
[35] I.M. Hafez, P.R. Cullis, Cholesteryl hemisuccinate exhibits pH sensitive polymorphic phase behavior, Biochim. Biophys. Acta - Biomembr. 1463 (2000) 107–114, https://doi.org/10.1016/S0005-2736(99)00186-8.
[36] W.X. Ding, X.R. Qi, P. Li, Y. Maitani, T. Nagai, Cholesteryl hemisuccinate as a membrane stabilizer in dipalmitoylphosphatidylcholine liposomes containing saikosaponin-d, Int. J. Pharm. 300 (2005) 38–47, https://doi.org/10.1016/j.ijpharm.2005.05.005.
[37] M.T. Liang, N.M. Davies, I. Toth, Encapsulation of lipopeptides within liposomes: Effect of number of lipid chains, chain length and method of liposome preparation, Int. J. Pharm. 301 (2005) 247–254, https://doi.org/10.1016/j.ijpharm.2005.06.010.
[38] A.H. De Vries, A.E. Mark, S.J. Marrink, The binary mixing behavior of phospholipids in a bilayer: A molecular dynamics study, J. Phys. Chem. B 108 (2004) 2454–2463, https://doi.org/10.1021/jp0366926.
[39] S. Esteban-Martín, J. Salgado, Self-assembling of peptide/membrane complexes by atomistic molecular dynamics simulations, Biophys. J. 92 (2007) 903–912, https://doi.org/10.1529/biophysj.106.093013.
[40] B. Orioni, G. Bocchinfuso, J.Y. Kim, A. Palleschi, G. Grande, S. Bobone, Y. Park, J. Il Kim, K.soo Hahm, L. Stella, Membrane perturbation by the antimicrobial peptide PMAP-23: A fluorescence and molecular dynamics study, Biochim. Biophys. Acta - Biomembr. 1788 (2009) 1523–1533, https://doi.org/10.1016/j.bbamem.2009.04.013.
[41] G. Bocchinfuso, A. Palleschi, B. Orioni, G. Grande, F. Formaggio, C. Toniolo, Y. Park, K.S. Hahm, L. Stella, Different mechanisms of action of antimicrobial peptides: Insights from fluorescence spectroscopy experiments and molecular dynamics simulations, J. Pept. Sci. (2009) 550–558, https://doi.org/10.1002/psc.1144.
[42] J.W. Essex, M.M. Hann, W.G. Richards, Molecular dynamics simulation of a hydrated phospholipid bilayer, Philos. Trans. R. Soc. B Biol. Sci. 344 (1994) 239–260, https://doi.org/10.1098/rstb.1994.0064.
[43] B. Sadanandan, V. Vaniyamparambath, K.N. Lokesh, K. Shetty, A.P. Joglekar, P. Ashrit, B. Hemanth, Candida albicans biofilm formation and growth optimization for functional studies using response surface methodology, J. Appl. Microbiol. 132 (2022) 3277–3292, https://doi.org/10.1111/jam.15402.
[44] L.F. Pacheco, D.B. Vieira, F.M. Correia, A.M. Carraona-Ribeiro, Interaction between cationic bilayers and Candida albicans cells, Prog. Colloid Polym. Sci. (2004) 175–177, https://doi.org/10.1007/b97059.
[45] G. Smistad, N.B. Nguyen, I.K. Hegna, S.A. Sande, Influence of liposomal formulation variables on the interaction with Candida albicans in biofilm; a multivariate approach, J. Liposome Res. 21 (2011) 9–16, https://doi.org/10.3109/08982101003629009.
[46] J.M.S. Loh, N. Adenwalla, S. Wiles, T. Proft, Galleria mellonella larvae as an infection model for group A streptococcus, Virulence 4 (2013) 419–428, https://doi.org/10.4161/viru.24930.
[47] M.J. Hope, M.B. Bally, G. Webb, P.R. Cullis, Production of large unilamellar vesicles by a rapid extrusion procedure. Characterization of size distribution, trapped volume and ability to maintain a membrane potential, BBA - Biomembr. 812 (1985) 55–65, https://doi.org/10.1016/0005-2736(85)90521-8.
[48] D.W. Fry, J.C. White, I.D. Goldman, Rapid separation of low molecular weight solutes from liposomes without dilution, Anal. Biochem. 90 (1978) 809–815, https://doi.org/10.1016/0003-2697(78)90172-0.
[49] M.M. Reif, P.H. Hünenberger, C. Oostenbrink, New interaction parameters for charged amino acid side chains in the GROMOS force field, J. Chem. Theory Comput. 8 (2012) 3705–3723, https://doi.org/10.1021/ct300156h.
[50] C. Margreitter, M.M. Reif, C. Oostenbrink, Update on phosphate and charged post-translationally modified amino acid parameters in the GROMOS force field, J. Comput. Chem. 38 (2017) 714–720, https://doi.org/10.1002/jcc.24733.
[51] I. Marzuoli, C. Margreitter, F. Fraternali, Lipid head group parameterization for GROMOS 54A8: a consistent approach with protein force field description, J. Chem. Theory Comput. 15 (2019) 5175–5193, https://doi.org/10.1021/acs.jctc.9b00509.
[52] Z.J. Frangos, K.A. Wilson, H.M. Aitken, R.C. Chater, R.J. Vandenberg, M.L. O'Mara, Membrane cholesterol regulates inhibition and substrate transport by the glycine transporter, GlyT2, Life Sci. Alliance 6 (2023) e202201708, https://doi.org/10.26508/lsa.202201708.
[53] H.J.C. Berendsen, J.P.M. Postma, W.F. van Gunsteren, J. Hermans, Interaction Models for Water in Relation to Protein Hydration, Intermol. Forces (1981) 331–342, https://doi.org/10.1007/978-94-015-7658-1_21.
[54] B. Hess, P-LINCS: a parallel linear constraint solver for molecular simulation, J. Chem. Theory Comput. 4 (2008) 116–122, https://doi.org/10.1021/ct700200b.
[55] S. Miyamoto, P.A. Kollman, Settle: an analytical version of the SHAKE and RATTLE algorithm for rigid water models, J. Comput. Chem. 13 (1992) 952–962, https://doi.org/10.1002/jcc.540130805.
[56] G. Bussi, D. Donadio, M. Parrinello, Canonical sampling through velocity rescaling, J. Chem. Phys. 126 (2007) 14101–14107, https://doi.org/10.1063/1.2408420.
[57] H.J.C. Berendsen, J.P.M. Postma, W.F. Van Gunsteren, A. Di Nola, J.R. Haak, Molecular dynamics with coupling to an external bath, J. Chem. Phys. 81 (1984) 3684–3690, https://doi.org/10.1063/1.448118.
[58] M. Parrinello, A. Rahman, Polymorphic transitions in single crystals: a new molecular dynamics method, J. Appl. Phys. 52 (1981) 7182–7190, https://doi.org/10.1063/1.328693.
[59] J.L. Rodriguez-Tudela, EUCAST definitive document EDef 7.1: method for the determination of broth dilution MICs of antifungal agents for fermentative yeasts, Clin. Microbiol. Infect. 14 (2008) 398–405, https://doi.org/10.1111/j.1469-0691.2007.01935.x.